How patch size and refuge availability change interaction strength and population dynamics: a combined individual- and population-based modeling experiment

Yuanheng Li[1,2,3], Ulrich Brose[1,2], Katrin Meyer[4] and Björn C. Rall[1,2]

[1] German Centre for Integrative Biodiversity Research (iDiv) Halle-Jena-Leipzig, Leipzig, Germany
[2] Institute of Ecology, Friedrich-Schiller Universität Jena, Jena, Germany
[3] Johann-Friedrich-Blumenbach Institute of Zoology and Anthropology, Georg-August-Universität Göttingen, Göttingen, Germany
[4] Department of Ecosystem Modelling, Georg-August-Universität Göttingen, Göttingen, Germany

ABSTRACT

Knowledge on how functional responses (a measurement of feeding interaction strength) are affected by patch size and habitat complexity (represented by refuge availability) is crucial for understanding food-web stability and subsequently biodiversity. Due to their laborious character, it is almost impossible to carry out systematic empirical experiments on functional responses across wide gradients of patch sizes and refuge availabilities. Here we overcame this issue by using an individual-based model (IBM) to simulate feeding experiments. The model is based on empirically measured traits such as body-mass dependent speed and capture success. We simulated these experiments in patches ranging from sizes of petri dishes to natural patches in the field. Moreover, we varied the refuge availability within the patch independently of patch size, allowing for independent analyses of both variables. The maximum feeding rate (the maximum number of prey a predator can consume in a given time frame) is independent of patch size and refuge availability, as it is the physiological upper limit of feeding rates. Moreover, the results of these simulations revealed that a type III functional response, which is known to have a stabilizing effect on population dynamics, fitted the data best. The half saturation density (the prey density where a predator consumes half of its maximum feeding rate) increased with refuge availability but was only marginally influenced by patch size. Subsequently, we investigated how patch size and refuge availability influenced stability and coexistence of predator-prey systems. Following common practice, we used an allometric scaled Rosenzweig–MacArthur predator-prey model based on results from our *in silico* IBM experiments. The results suggested that densities of both populations are nearly constant across the range of patch sizes simulated, resulting from the constant interaction strength across the patch sizes. However, constant densities with decreasing patch sizes mean a decrease of absolute number of individuals, consequently leading to extinction of predators in the smallest patches. Moreover, increasing refuge availabilities also allowed predator and prey to coexist by decreased interaction strengths. Our results underline the need for protecting large patches with high habitat complexity to sustain biodiversity.

INTRODUCTION

The interplay between stability, complexity and biodiversity of ecological networks (especially food webs) is a subject of a long lasting and still ongoing discussion in ecology (e.g., *MacArthur, 1955*; *May, 1972*; *McCann, 2000*). From a mathematical point of view, an increase of species richness is only possible when the interaction strength between the species in a network (i.e., the strength of feeding interactions in a food web) decreases (*May, 1972*), otherwise species richness (represents biodiversity) must decline. A few possible solutions to overcome this problem have already been proposed, including a non-random organization of the feeding links in real food webs (*Yodzis, 1981*) and a decrease of specific interaction strength with increasing trophic levels (*De Ruiter, Neutel & Moore, 1995*), both driven by allometry (*Yodzis & Innes, 1992*; *Brose, Williams & Martinez, 2006*; *Otto, Rall & Brose, 2007*). Classic stability analyses assumed that the strength of interactions (the functional response) increased linearly with increasing resource availability (e.g., *May, 1972*). In food web studies, interaction strength refers to feeding interactions, which can be studied by investigating the 'functional response': how the number of prey eaten by a predator changes with increasing prey densities. In his seminal work, *Holling (1959b)* described the mechanism of functional responses mathematically and showed that under the simplest assumptions it should follow a hyperbolic curve. This experiment was performed in a simple experimental trial with blindfolded students (the predator) on a plain nine-square foot table as the experimental arena and sandpaper discs as prey. Interestingly, already in the same year *Holling (1959a)* showed that the shape of functional response could also follow a sigmoid (i.e., s-shaped) curve when investigating small mammals on a large natural scale, including natural complexity in the habitat. The different possible shapes of functional responses are known as type I functional responses (linear with a limit), type II functional responses (hyperbolic) and type III functional responses (sigmoid), forming the core set of functional responses alongside a number of other descendant types (*Jeschke, Kopp & Tollrian, 2002*). Notably, it has been shown that the type I functional response is an artifact (*Jeschke, Kopp & Tollrian, 2004*; *Sarnelle & Wilson, 2008*), so in this study we focus only on the non-linear functional responses. One of the descendants of Holling's functional response models based on enzyme kinetics (*Real, 1977*) unifies the type II and the type III functional responses:

$$f(N) = \frac{f_{max}N^h}{N_0^h + N^h} \tag{1}$$

where $f(N)$ is the per capita feeding rate, depending on the resource density, N. The curve is characterized by a maximum feeding rate, f_{max} [# h^{-1}]; a half saturation density, N_0 [# m^{-2}], i.e., the prey density when the predator's feeding rate reaches half of the maximum feeding rate and a unitless Hill exponent, h, determining the curve shape. If

the Hill exponent is set to unity, the resulting function is the "strict" type II functional response. Whereas if the Hill exponent is set to two, it is the "strict" type III functional response in a very classical sense (but see *Juliano (2001)* for alternative descriptions of the type III functional response). We will subsequently refer to any functional responses as type III functional responses if the Hill exponent is larger than unity.

But why is it so important to know if the functional response is a type II functional response or a type III functional response? The answer is that type III functional responses are known to stabilize population dynamics thereby allowing for persistence of large food webs (*Williams & Martinez, 2004*; *Brose, Williams & Martinez, 2006*; *Rall, Guill & Brose, 2008*), by regulating prey populations to low densities (*Nunney, 1980a*; *Nunney, 1980b*). Several mechanisms have been put forward to explain why a type III functional response should appear, including the predator learning to exploit prey better (*Holling, 1966*) and switching between different prey types to the most abundant prey (*Murdoch & Oaten, 1975*; *Oaten & Murdoch, 1975*). More recently, it was suggested that refuges for the prey can also lead to a type III functional response (e.g., *Scheffer & De Boer, 1995*; *Vucic-Pestic et al., 2010a*). However, there was only mixed support from studies manipulating habitat complexity in general without introducing prey refuges explicitly (*Kaiser, 1983*; *Hoddle, 2003*; *Hohberg & Traunspurger, 2005*; *Hauzy et al., 2010*; *Vucic-Pestic et al., 2010a*; *Kalinkat, Brose & Rall, 2013*). Those differences may be caused by variations in how habitat complexity influences foraging and hence feeding: (1) complexity negatively affects feeding by e.g., refuges restraining predation especially at low prey densities and eventually leading to a type III functional response; (2) it affects feeding by e.g., obstacles preventing the movements of both predator and prey leading to reduced encounter rates at all prey densities but leaving the functional response type unaffected (*Hauzy et al., 2010*). Moreover, if the habitat complexity influences neither movement nor refuge provision, it will simply cause a dilution effect, a virtual increase of the patch size (*Kalinkat, Brose & Rall, 2013*).

Furthermore, functional response studies are predominantly carried out under artificial laboratory conditions (*Jeschke, Kopp & Tollrian, 2004*; *Kalinkat & Rall, 2015*). This means that (1) most of the studies mentioned above have used rather artificial habitat complexity and (2) due to spatial limitations of a laboratory, the size of the experimental units are relatively small (e.g., petri-dishes for estimating the functional response of ladybugs, *Stethorus japonicus* (*Gotoh, Nozawa & Yamaguchi, 2004*)). Only a few studies have attempted to investigate functional responses in natural environments, but these studies are only roughly comparable to the controlled laboratory studies as they rely on scat counting or gut content analyses combined with assessments of natural prey density (e.g., *Dale, Adams & Bowyer, 1994*; *Smout & Lindstrøm, 2007*). To our knowledge, only one study so far has investigated and compared the simplified laboratory functional response experiments (using petri dishes) with functional responses measured in the greenhouse or in the field (*Munyaneza & Obrycki, 1997*). In this study, the attack rates in the laboratory were over 40 times higher than those in the greenhouse but those in the field were three to nine times lower than in the petri dishes (note that all functional responses in the original publication were fitted to a type II functional response model and the attack rates were scaled to the total size of the experimental arena, we compared

the attack rates scaled to square meters (*Rall et al., 2012*)). As the experiments carried out by *Munyaneza & Obrycki (1997)* altered habitat complexity and patch size at the same time, and both gradients increased simultaneously from the petri dish experiments over the greenhouse to the field experiments, it was not possible to disentangle the potential interactive effect of habitat complexity and patch size. Furthermore, *Bergström & Englund (2004)* reported increases in attack rates with patch size, and studies manipulating habitat complexity reported a decrease in attack rates (e.g., *Vucic-Pestic et al., 2010a*). This might lead to the explanation that the relatively low attack rates in the field shown in the study of Munyaneza & Obrycki were due to the increased patch size and habitat complexity.

Beside the examples above, we are not aware of any other study addressing the effect of patch size and habitat complexity on the functional-response parameters. Moreover, most of the studies only vary habitat complexity or patch size by up to four levels (e.g., *Kalinkat, Brose & Rall, 2013*; *Bergström & Englund, 2004*) and none of them systematically varied both complexity and size. This lack of studies is perhaps due to the laborious nature of functional response studies. For example, *Vucic-Pestic et al. (2010b)* used prey ranging from one up to 4,000 individuals for fitting a single functional response, measuring up to 90 feeding experiments. Doubling the patch size would already lead to a maximum of 8,000 individuals and a 10 times larger patch would require already a maximum of 40,000 individuals.

As such extreme laboratory settings are not feasible, we developed an individual-based model (IBM) to study the effects of patch size and refuge availability on functional-response parameters. We explored full-factorial patch size and habitat complexity to disentangle effects of both variables and eventually their interactive effects on the functional-response parameters. Subsequently, we analyzed the stability of a predator-prey system depending on patch size and habitat complexity by developing a predator-prey population dynamics model which has a long standing usage and wide applicability (see section "Methods" for details).

METHODS

Individual-based model of feeding interaction
Overview
To investigate the effects of patch size and habitat complexity (represented by refuge availability) on functional-response parameters, we developed an individual-based allometric predator-prey model (for details, see the supplement for an **O**verview, **D**esign concepts, **D**etail protocol, *Grimm et al. (2006)*; *Grimm et al. (2010)*) to mimic the feeding experiments in the laboratory. We assumed that the maximum feeding rate was driven by mechanical and physiological processes such as chewing and digestion and would not scale with patch size or refuge availability. Therefore, we first investigated the maximum feeding rate without any explicit space properties. Second, we modeled a two-dimensional square area to mimic an explicit patch in which both predator and prey can continuously move. The modeled patch consisted of cells all individuals can enter; however, cells may be marked as refuges preventing predation.
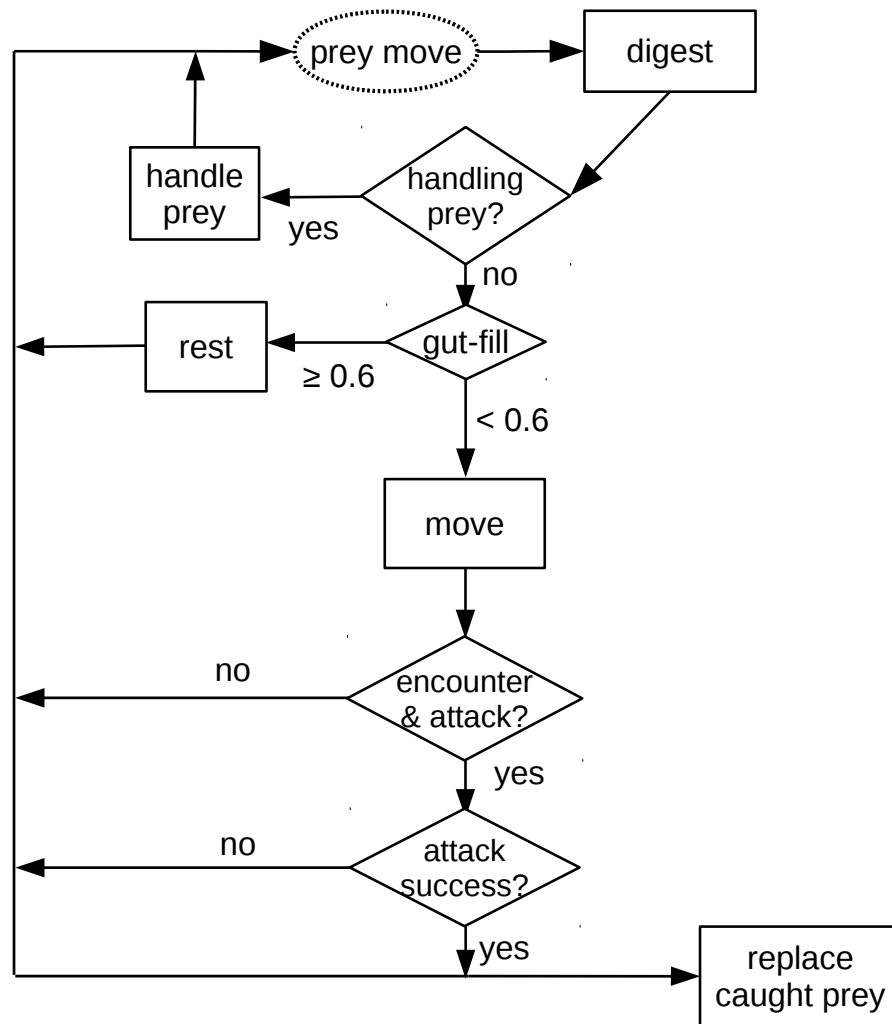
Figure 1 Schematic diagram of processes in the *in silico* feeding experiment model. The text in the dashed oval is the only prey action which is also the start of the processes. Texts in the squares are decisions or actions of the predator. Texts in the diamonds are decisions making, e.g., "handling prey?"

The model processes

The first process applied in the model is prey movement (random walk with randomly chosen direction, 0–2π double precision floating number and allometrically calculated distance). The following processes applied in the model are all decisions and actions of the predator (Fig. 1). First, the digestion of the predator is calculated. Subsequently, the algorithm checks if the predator is handling prey (caught in an earlier time step). If not, and the predator's gut is full ($\geq 60\%$), it rests (not taking further actions). If the predator is not handling prey and is hungry (gut filling $< 60\%$), the predator moves (random walk, see above). After reaching the new position, the predator investigates if it encounters a prey in the cell. If there is a prey individual in the same cell, it will be attacked. If the attack is successful, another prey item is placed randomly into the grid to keep the prey density constant. The predator starts to handle (chew) prey in the next time step.

Variables and parameters

Most species traits regulating the processes described above follow allometric rules (*Kleiber, 1961*; *Peters, 1983*; *Brown et al., 2004*; *Brose, 2010*), including velocity, V [cm s^{-1}], of both the predator and the prey (*Peters, 1983*); and the traits of the predator: gut size, G [mg] (*Ibarrola et al., 2012*), digestion rate, D [mg s^{-1}] (*Ibarrola et al., 2012*), handling time, T_h [s] (estimated from *Rall et al., 2012*, see Supplemental Information) and attack success, S_a [unitless] (*Brose et al., 2008*; *Gergs, 2011*):

$$V = v_0 M^{a_v} \tag{2a}$$

$$G = g_0 M^{a_g} \tag{2b}$$

$$D = d_0 M^{a_d} \tag{2c}$$

$$T_h = h_0 M_p^{a_{h,p}} M_n^{a_{h,n}} \tag{2d}$$

$$S_a = a_0 \left(\frac{R}{R_{opt}} e^{1 - \frac{R}{R_{opt}}} \right)^{\lambda} \tag{2e}$$

where v_0, g_0, d_0 and h_0 are constants, a_v, a_g, a_d and a_h are the allometric scalings, and M is the body mass of the corresponding individual. Subscripts, $_p$ and $_n$ indicate predator and prey respectively. We used the widespread generalized Ricker's function (*Persson et al., 1998*; *Persson & Brönmark, 2002b*; *Persson & Brönmark, 2002a*; *Wahlström et al., 2000*; *Brose et al., 2008*; *Rall et al., 2011*) to describe the scaling of attack success depending on body mass. This function consists of the maximum attack success a_0, predator-prey body-mass ratio, R and its optimum R_{opt} and a shaping parameter, λ. Predator and prey also possessed some state variables to assist their decision making and activities, i.e., the 'position' for all individuals; the 'gut fullness' and if the predator is 'still handling' and an identifier, 'prey identity,' to distinguish between the prey individuals.

Parameters' range

The cell resolution of the square grid, in which the *in silico* simulations are conducted is 1 cm × 1 cm. As we intended to mimic laboratory experiments, the walls of the grid are set to 'wall-boundary condition' (individuals cannot penetrate the walls). We chose twelve patch sizes ranging from 0.2 m × 0.2 m = 0.04 m^2 (the size of a standard patch in some terrestrial functional response experiments (*Brose et al., 2008*; *Rall et al., 2010*; *Vucic-Pestic et al., 2010a*; *Rall et al., 2011*; *Vucic-Pestic et al., 2011*; *Kalinkat, Brose & Rall, 2013*) to 100 m^2 (the size of a field patch (*Munyaneza & Obrycki, 1997*)). The sizes of each patch were: 0.04 m^2, 0.16 m^2, 0.64 m^2, 1.44 m^2, 2.56 m^2, 4 m^2, 16 m^2, 36 m^2, 49 m^2, 64 m^2, 81 m^2, and 100 m^2. The second independent variable we modeled was prey refuge that served as a surrogate for habitat complexity which preventing feeding. We randomly selected refuge cells on the grid for each simulation in a certain percentage of cells in steps of 5% (5%–75% as the ratio of refuge cells to all cells); see Fig. 2 as a case example. These two independent variables are full-factorially simulated. For each simulation run, the refuge distribution is newly drawn. Those randomly chosen cells do not support any feeding by the predator and therefore act as refuges for the prey. The body masses of the predator and prey were set to 100 mg and 1 mg, a common body-mass ratio for animal predatory interactions, close to
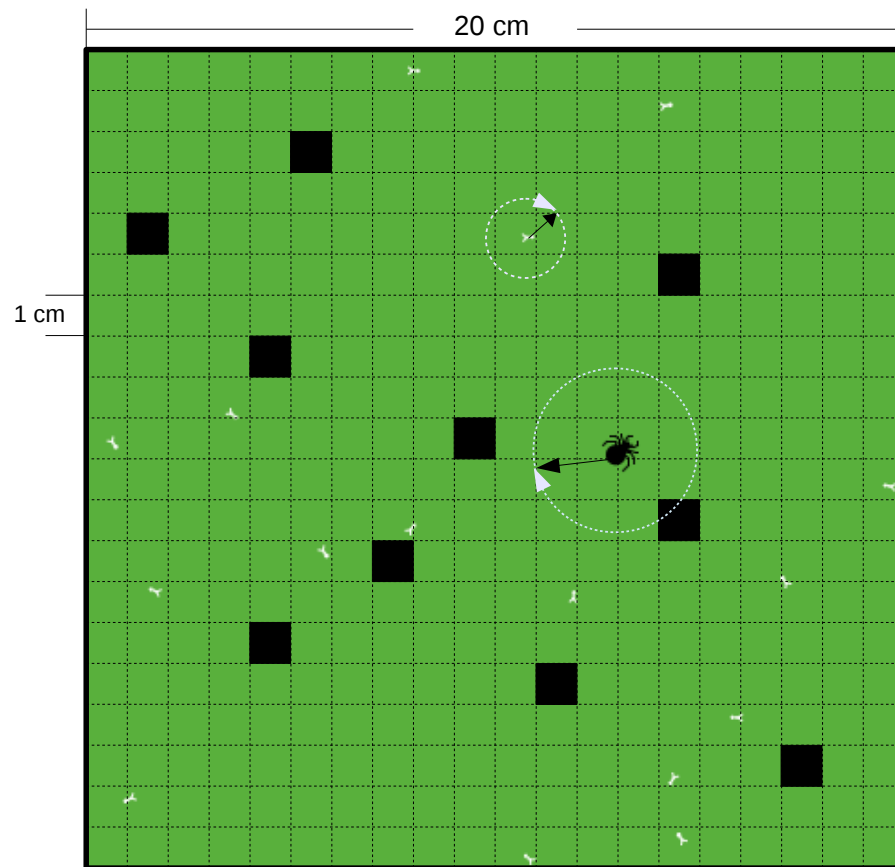
Figure 2 Schematic diagram of a square grid of the IBM model. The grid in this example is 0.04 m² with cell resolution of 1 cm × 1 cm and with a 'wall-boundary condition' (individuals not able to penetrate the walls). The black cells are the refuge cells. The small white bugs represent prey and the big black bug represents the predator. The random walk of the individuals is decided by a randomly chosen direction, 0–2π and an allometrically decided distance (as denoted by the white circles and black arrows).

the optimal feeding ratio of invertebrates (e.g., *Vucic-Pestic et al., 2010b*; *Rall et al., 2011*; *Kalinkat et al., 2013*). We ran each of the *in silico* feeding trials for 3,600 steps (representing 1 h). The simulation for estimating the maximum feeding rate was repeated 50 times and each prey density dependent simulation was repeated five times. We simulated prey densities from 2^0 to 2^n as the density when the predator (only one predator per simulation) is satiated. For example, twenty prey densities from 2^0 to 2^{19} are selected for the patch size of 36 m² and 35% refuge-area ratio. Values for the parameters in allometric equations, Eq. (2), are empirically-based and given in Table 1. These values (Table 1) are derived from the same studies where we derived the formulas. Yet the maximum attack success a_0 is taken as the mean of 5 measurements from *Gergs (2011)*. The optimum predator-prey body-mass ratio is consistent with terrestrial invertebrates from *Brose et al. (2008)*.

Table 1 Parameters values in allometric equations (Eq. (2)).

Parameter	Value	Parameter	Value
v_0	0.546	a_v	0.29
g_0	0.50	a_g	0.434
d_0	5×10^{-5}	a_d	0.75
h_0	37.504	$a_{h,p}$	-0.330
		$a_{h,n}$	0.173
a_0	0.10	R_{opt}	100
		λ	1

Statistics
Functional response fitting

We first calculated the mean maximum feeding rate for the predator-prey pair. We used a generalized linear model (GLM) assuming that maximum feeding rates follow Poisson distribution as feeding rates were count data of non-negative integers of which the error distribution increases with increasing mean. The statistics were ran in R (*R Core Team, 2016*), but see chapter 13 in *Crawley (2007)* for details. Subsequently, we used this mean maximum feeding rate as a fixed parameter in the functional response model (Eq. (1)) to estimate the dependencies of the remaining half saturation density and Hill exponent.

We analyzed the feeding data from IBM models using Real's functional response, Eq. (1). As there is no well-established scaling relationships of functional-response parameters (half saturation density and Hill exponent) to habitat properties investigated here, i.e., patch size and refuge availability, we preliminarily tested whether the scalings of these functional-response parameters followed a power law or exponential function. To reduce the potential influences of interaction terms (between patch size and refuge availability) which may influence the dependencies of the half saturation density or Hill exponent, we included all interaction terms in the preliminary testing (*Zuur et al., 2009*). We analyzed in total 16 full models and compared them using the Bayesian Information Criterion (BIC), see Table S3. This analysis revealed that the scalings of half saturation densities with patch size and refuge availability can be best described by a power law and an exponential function, respectively:

$$N_0 = C_{N_0} \, A^{a_{N_0}} \, e^{b_{N_0} R} \, e^{\gamma_{N_0} \ln(A) R} \tag{3}$$

where C_{N_0} is a constant, a_{N_0} is the scaling exponent of half saturation density to patch size, A, b_{N_0} is the scaling parameter of half saturation density to refuge availability, R and γ_{N_0} is the parameter giving the strength of the interaction between patch size and refuge availability. Preliminary analyses also showed that the Hill exponent depended on patch size and refuge availability both following power laws:

$$h = C_h \, A^{a_h} \, R^{b_h} \, e^{\gamma_h \ln(A) \ln(R)} \tag{4}$$

where C_h is a constant, a_h is the scaling parameter of the Hill exponent to patch size, A, b_h is the scaling exponent of the Hill exponent to refuge availability, R and γ_h is the parameter giving the strength of the interaction between patch size and refuge availability.

We fitted the functional response model, Eq. (1) with the dependencies described above using a maximum likelihood method, 'mle2()' (*Bolker & R Development Core Team, 2014*), (see *Bolker (2008)* for details). As we replaced eaten prey after each feeding event (see above), we assumed that the residuals followed a negative binomial distribution. We fitted this functional response model to the data assuming a log link between data and model:

$$\ln(N_0) = \ln\left(C_{N_0}\right) + a_{N_0}\ln(A) + b_{N_0}R + \gamma_{N_0}\ln(A)R \qquad (5a)$$

$$\ln(h) = \ln(C_h) + a_h\ln(A) + b_h\ln(R) + \gamma_h\ln(A)\ln(R) \qquad (5b)$$

i.e., we did not fit the values for the constants C in Eqs. (3) and (4), but for the intercepts in the ln-transformed version $\ln(C_{N_0})$ and $\ln(C_h)$ in Eq. (5). We performed a model selection using the Bayesian Information Criterion (BIC) by comparing all possible combinations of setting the parameters a, b and γ to "0," resulting in 25 meaningful combinations (note that either a or b only can be excluded if the interaction term, γ is excluded).

Population dynamics model

To investigate how patch size, A, and refuge availability (a measurement of habitat complexity), R, affect population dynamics and stability of a predator-prey system, we set up an ordinary differential equations (ODE) model. Such models were widely used to study one population (e.g., *Gompertz, 1825*; *Verhulst, 1838*) over food web motifs (e.g., *Lotka, 1925*; *Volterra, 1926*; *Rosenzweig & MacArthur, 1963*; *Rosenzweig, 1971*; *Yodzis & Innes, 1992*) to multi-trophic food web models (e.g., *Williams & Martinez, 2004*; *Binzer et al., 2016*; *Schneider et al., 2016*) and used to predict patterns of experimental microcosms (e.g., *Schneider, Scheu & Brose, 2012*; *Fussmann et al., 2014*) up to whole food webs (e.g., *Boit et al., 2012*). The ODE model describes the change in prey density [# m^{-2}], dN, and predator density [# m^{-2}], dP, over time, dt (*Rosenzweig & MacArthur, 1963*; *Yodzis & Innes, 1992*; *Otto, Rall & Brose, 2007*):

$$\frac{dN}{dt} = rN\left(1 - \frac{N}{K}\right) - \omega\frac{f_{max}N^h}{N_0^h + N^h}P \qquad (6)$$

$$\frac{dP}{dt} = e\omega\frac{f_{max}N^h}{N_0^h + N^h}P - xP \qquad (7)$$

where the prey growth is described by logistic growth with r [d^{-1}] being the intrinsic growth rate and K [# m^{-2}] being the carrying capacity. The prey are consumed by the predator following Real's functional response, Eq. (1), with f_{max} being the maximum feeding rate, N_0 being the half saturation density and h being the Hill exponent. The predator population grows according to the functional response multiplied by the assimilation efficiency, e, and the effective foraging time proportion ω. Moreover, it loses population density by metabolism, x [d^{-1}].

We used the estimated values from the functional response fitting of our individual-based model (see above) in the ODEs. Additionally we calculated the values for carrying capacity, K, growth rate, r and metabolism, x, according to empirically derived studies (*Rall et al., 2010*; *Meehan, 2006*; *Savage et al., 2004a*; *Peters, 1983*) (details described afterwards).

Equilibrium densities of the predator-prey system and extinction boundaries

The predator-prey population model has a set of non-trivial analytical solutions, being a predator isocline

$$N = \left(\frac{x N_0{}^h}{e\omega f_{max} - x} \right)^{\frac{1}{h}} \tag{8}$$

and a prey isocline

$$P = r N^{1-h}(k - N) \frac{N_0{}^h + N^h}{k\omega f_{max}}. \tag{9}$$

After obtaining these isoclines, the equilibrium densities of predator and prey are compared with extinction boundaries [# m^{-2}]. Such boundary is set to an artificial small number in the common practice of ODE models, but we explicitly set it to two individuals per patch. In cases where the predator population is not sustained, i.e., the equilibrium density is less than the extinction boundary, prey population would grow to its capacity, $N = K$ and the predator population goes extinct, $P = 0$.

Parameter values for the ODE

The functional-response parameters, the maximum feeding rate, f_{max}, the half saturation density, N_0 and the Hill exponent, h, are set according to the statistical results of the IBM simulations. We assumed that the predator foraged approximately 12 h a day (*Ebeling & Bray, 1976*), therefore we added a foraging time proportion $\omega = \frac{1}{2}$. The assimilation efficiency, e, accounts for the proportion of food overwhelmed by the predator which can be converted to its own body mass, which is set to 0.85, a common value for predatory consumers (*Yodzis & Innes, 1992*; *Otto, Rall & Brose, 2007*). The prey growth follows the logistic growth consisting of the intrinsic growth rate r and the carrying capacity K. Together with metabolic rate of the predator, these three parameters are calculated by empirically derived equations.

$$K = K_0 M_n^{b_K} e^{\frac{E_K}{kT}} \left(\sigma_0 e^{\frac{E_\sigma (T_0 - T)}{kT T_0}} \right)^z e^{t l_0 (tl - 1)} \tag{10a}$$

$$r = r_0 M_n^{b_r} e^{\frac{E_r}{kT}} \tag{10b}$$

$$x = \sigma c_x x_0 M_p^{b_x} e^{\frac{-E_x}{kT}} \tag{10c}$$

The carrying capacity K scales with body mass, M_n (gram), environmental temperature, T (K), net primary production of the habitat, $\left(\sigma_0 e^{\frac{E_\sigma (T_0 - T)}{kT T_0}} \right)^z$, and the trophic level of the prey, tl. The values for all parameters are derived for invertebrate detritivores assuming German weather conditions and productivity: $K_0 = e^{-31.15}$; $b_K = -0.72$; $E_K = 0.71$; $k = 8.62e - 05$; $T = 282.65$; $\sigma_0 = 600$; $E_\sigma = -0.35$; $T_0 = 293.15$; $z = 1.03$; $tl_0 = -2.68$; $tl = 1.5$ (see *Meehan (2006)* and *Rall et al. (2010)* for details). The growth rate r, scales with body mass (microgram) and environmental temperature, where $r_0 = e^{32.39}$, $b_r = -0.25$ and $E_r = -0.84$ (details see *Savage et al. (2004a)* and *Rall et al. (2010)*). The metabolic rate x, also scales with body mass (gram) and environmental temperature with $x_0 = e^{27.68}$, $b_x = 0.72$ and $E_x = 0.87$ (see *Peters (1983)*; *Savage et al. (2004b)* and *Rall et al. (2010)* for details). *Savage et al. (2004b)* reported that field metabolic rate were three times larger

Li et al. (2017), *PeerJ*, DOI 10.7717/peerj.2993

10/22

Table 2 Statistical results for the *in silico* functional response experiments. Note that the maximum feeding rate is a priori assumed to be independent of patch size and refuge availability.

		Estimate	S.E.	*p*-value
Maximum feeding rate	$\ln(f_{max})$	1.902	0.05	<0.001
Half saturation density	$\ln(C_{N_0})$	4.577	0.031	< 0.001
	a_{N_0}	−0.007	0.005	0.21
	b_{N_0}	1.777	0.063	< 0.001
	γ_{N_0}	Excluded by model selection		
Hill exponent	$\ln(C_h)$	0.25	0.011	< 0.001
	a_h	Excluded by model selection		
	b_h	Excluded by model selection		
	γ_h	Excluded by model selection		

than basal, therefore we include the coefficient σ as 3. The normalization constant c_x, 12342.86 M_p^{-1} (M_p in milligram), converts the metabolism from J s^{-1} to d^{-1} (*Peters, 1983*).

We set predators to 100 mg, and prey to 1 mg, consistent with our individual-based model simulations described above. We also explored the same ranges of patch size and habitat complexity as for the individual-based model simulations explained above. Extinction boundaries for predator and prey were set to two individuals per patch.

RESULTS

Results of IBM simulation

The maximum feeding rate, f_{max}, was estimated prior to the functional response fitting and revealed that predators of 100 mg fed in average 6.7 prey individuals per hour (Table 2, note that the statistics were performed using a log-link function, i.e., the ln-linear feeding rate was estimated). We subsequently fitted the functional response with a fixed maximum feeding rate. Our model comparison of patch size and refuge availability dependent functional response models, based on BIC, included a scaling of half saturation density with patch size and refuge availability, but it did not include any scaling of the Hill exponent with either parameter (Table 2). The half saturation density increased with refuge availability, and decreased marginally with patch size, see Fig. 3. The estimated Hill exponent across patch sizes and refuge availabilities was 1.284, which is significantly different from a Hill exponent of 1 therefore indicating a type III functional response (Table 2, note that the ln-transformed Hill exponent was tested against "0" what is a Hill exponent of "1"). The emerging functional responses are of the same shape but feeding is realized at higher prey densities with increasing refuge availability (Fig. 4). Other predator-prey body-mass ratios showed similar results, see the section "*In silico* feeding experiments on other body-mass ratios" in the supplement.

Results of population dynamic model

We solved the population dynamics model by a set of analytical solutions (Eqs. (8) and (9)) and the extinction boundaries. In small patches only the prey species survived, but refuge availability relaxed this pattern, allowing predators to survive at smaller patches.
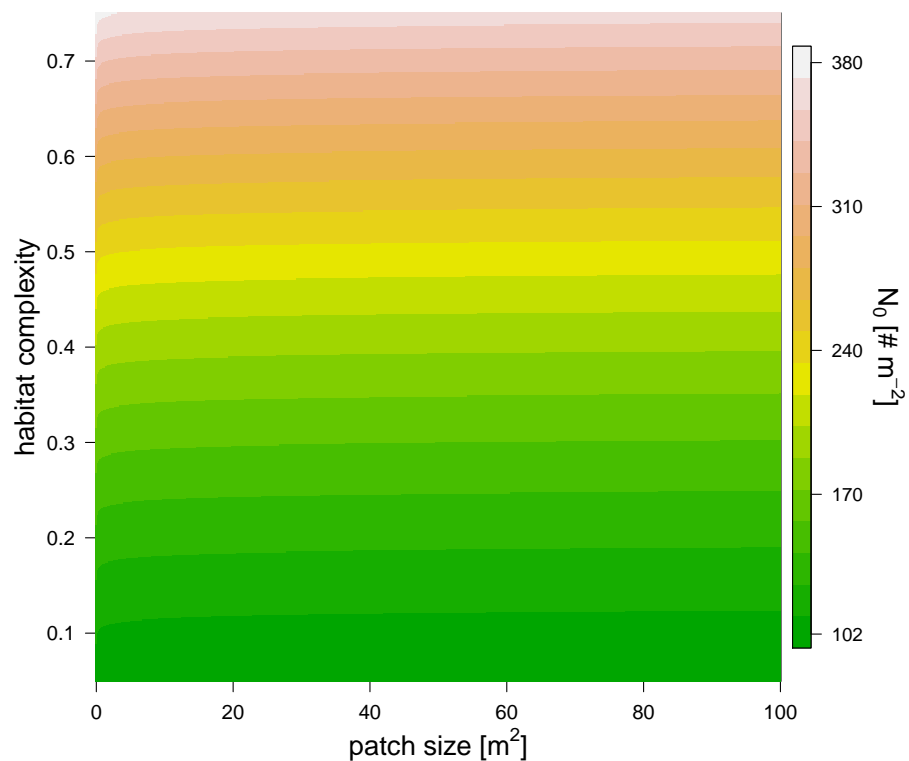
Figure 3 The effect of patch size (*x*-axis) and refuge availability (*y*-axis) on half saturation density (see color scale).

Both predator and prey population densities increased with refuge availability, whereas in larger patches, the densities of predator and prey populations decreased slightly (Fig. 5).

DISCUSSION

Effects of spatial properties on interaction strength

We developed an allometric individual-based model to investigate the effects of patch size and habitat complexity (represented by refuge availability) on feeding interactions. We found that the interaction strength decreased with refuge availability, as the half saturation density increased with it. This result is consistent with most of empirical studies aiming to account for how refuges affect predation rates (e.g., *Kaiser, 1983*; *Folsom & Collins, 1984*; *Kalinkat, Brose & Rall, 2013*). Our results showed that patch size, however, did not significantly influence the interaction strength. *Bergström & Englund (2004)* reported that the attack rate (the maximum interaction strength at low prey densities) increased with patch size. This increase was explained by behavioral changes in moving activity (increasing speed of the predator) and an aggregative behavior of both their prey and predator at the walls of their experimental aquariums (animals clustered more at the aquarium walls with increasing patch size). We did not include such behavioral changes in our model as we wanted to provide a simple basic model in this study, which may explain the differences of our results from *Bergström & Englund (2004)*. The Hill exponents in our *in silico* individual-based experiments were 1.28 across patch sizes and refuge availabilities.
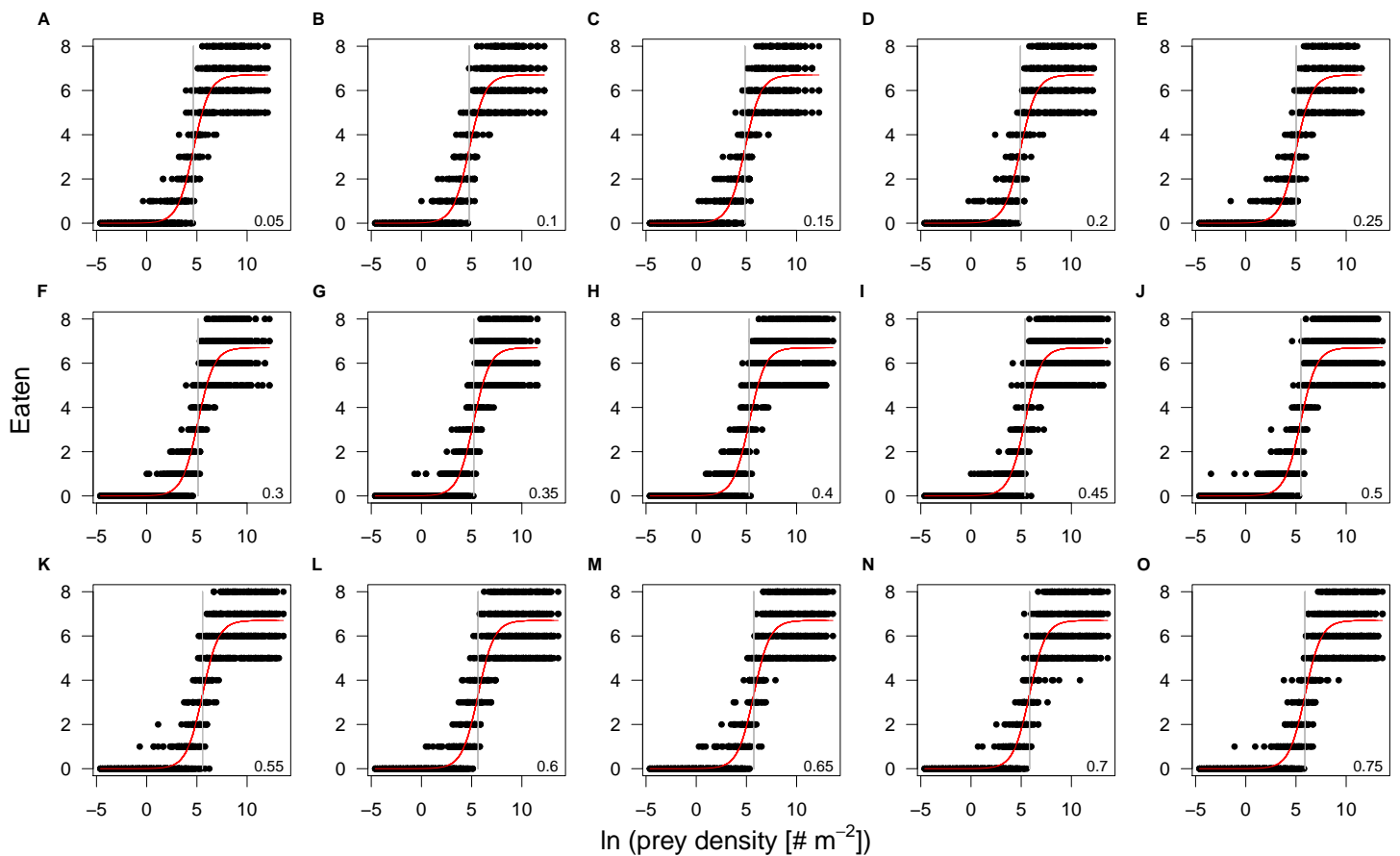
Figure 4 **Results of the individual-based functional response *in silico* experiments (black dots) and their corresponding fits (red lines).** The panels are arranged by increasing refuge availability, starting at 5% (A) to 75% (O). The patch size effect on the half saturation density is too small to result in visually distinguishable regression lines. All prey densities are ln-transformed. The grey vertical lines denote the half saturation densities.

This is quite surprising, as a simple type II functional response was thought to be the appropriate model for feeding interaction experiments under simplified conditions in the laboratory. However, the empirical findings of *Sarnelle & Wilson (2008)* suggested that type III functional responses would emerge if researchers were able to include experimental trials on small prey densities, which was not feasible for experiments carried out in small patches. A few feeding interaction studies on mammals ('intelligent predators') carried out in the field also suggested type III functional responses (*Holling, 1959a*; *Smout & Lindstrøm, 2007*). More recent studies found type III functional responses for invertebrates as well (*Aljetlawi, Sparrevik & Leonardsson, 2004*; *Vucic-Pestic et al., 2010b*). Our study not only corroborates the finding of type III functional response, but also confirms that for the mechanistically simplified predators as in our individual-based model, a type III functional response is appropriate, which is not only suitable for 'intelligent predators' with the ability to learn (*Holling, 1966*). The statistical results for *in silico* experiments of other body-mass ratios showed consistency with the results discussed above.

Former laboratory experiments that compared a homogeneous habitat with a complex habitat documented a shift from a type II to a type III functional response (*Vucic-Pestic*
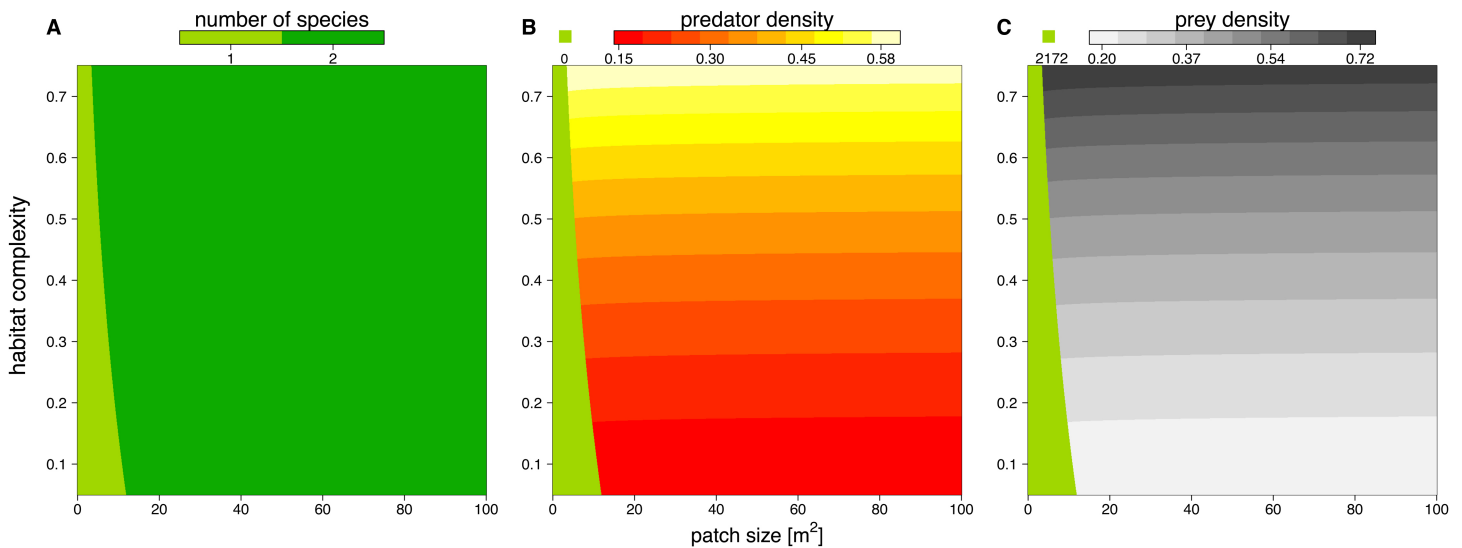
Figure 5 **Number of surviving species (A), population densities of predator (B) and prey (C) depending on patch size (*x*-axis) and refuge availability (*y*-axis).** When the system is embedded in very small patches, the predator becomes extinct due to energy limitation and the prey grows to its carrying capacity (green areas in B and C). The non-green areas of B and C show the densities, [# m^{-2}], of predator and prey when the system is feasible (see color code above each plot).

et al., 2010a) and argued that this was due to a refuge effect. We did, however, not find any increase in the Hill exponent with increasing refuge availability. As we did not include explicit behaviors for hiding, we infer that this switch from a type II to a type III functional response (or an increase of the Hill exponent) not only needed refuges as shelter for the prey, but also active behavioral changes in sub-habitat choice (*Schmitz, Krivan & Ovadia, 2004*; *Miller, Ament & Schmitz, 2014*).

Our individual-based predator-prey model framework allowed us to investigate the effects of patch size and refuge availability on functional-response parameters, which would not have been possible in laboratory or field experiments. Even without incorporating more complex movement models than random walks or behaviors like chasing or hiding, we were able to detect general patterns on the scalings of functional-response parameters with increasing patch size and refuge availability. Nevertheless, future individual based predator-prey models should incorporate more complex movement models to better understand the mechanisms of functional responses.

Effects of spatial properties on population dynamics

To investigate how changes in interaction strength scale up to population dynamics and coexistence, we analyzed a predator-prey ordinary differential equation model. We used the results from our *in silico* feeding experiments and combined it with empirically measured values for growth, carrying capacity and metabolism (*Meehan, 2006*; *Savage et al., 2004a*; *Savage et al., 2004b*; *Brown et al., 2004*; *Rall et al., 2010*). Increasing patch size turned the extinction of predators to survival, meaning the smallest patches were not able to sustain the predator population. This is surprising as the feeding interaction strength does not change with patch size (i.e., a non-significant effect of patch size). As all parameters of
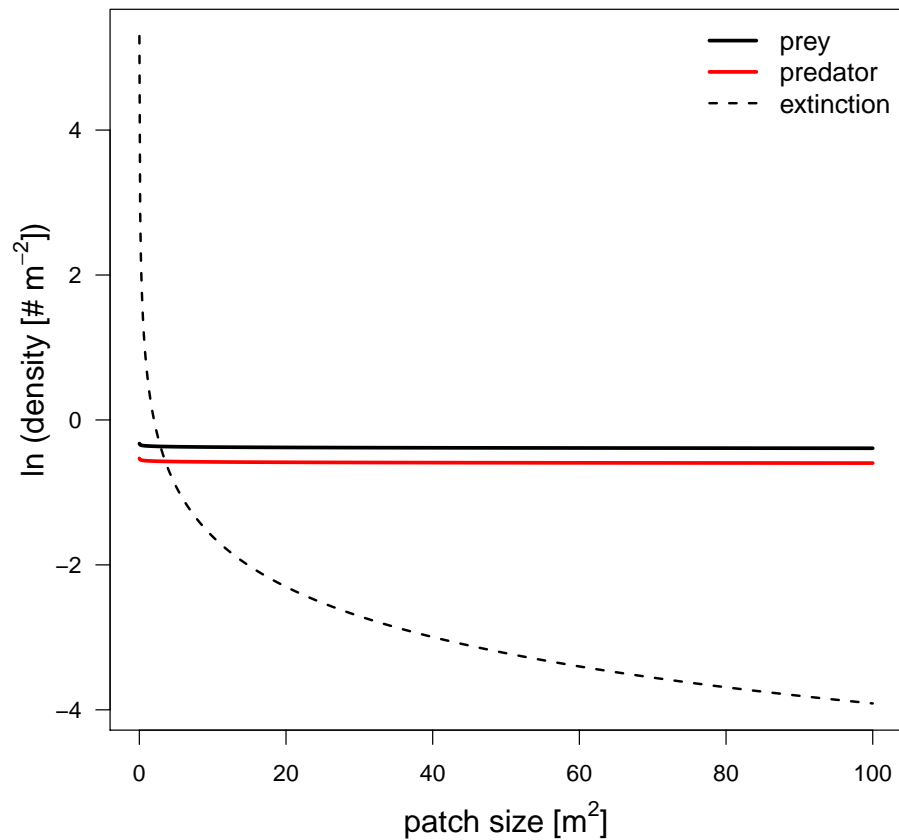
Figure 6 Equilibrium densities and extinction boundaries of the predator-prey system. This is an example where 73% of the cells are prey refuges. The solid lines depict the equilibrium population densities of the predator (red) and prey. The dashed line indicates the extinction boundaries of the predator and prey, two individuals per patch.

the model are constant in respect to patch size, we expected that neither the stability (*sensu* population dynamics) nor persistence will be affected. This paradox behavior of the system can only be explained by the increasing extinction thresholds with decreasing patch size. We defined the extinction threshold as two individuals per patch leading to increasing densities for extinctions with decreasing patch size (see Fig. 6 as an example). Increasing refuge availability counteracted this pattern and allowed predators to survive at even smaller patches. This is surprising as the half saturation density increased with refuge availability, suggesting less energy intake by the predator. However, increasing half saturation density also led to an increase in prey density in equilibrium that subsequently sustained a higher predator density. Both predator and prey have been feasible in larger patches and across the range of habitat complexities we explored.

Using a predator-prey population dynamics model, parameterized by the *in silico* functional response experiments discussed above, we were able to detect patterns of coexistence when patch size and refuge availability increased. These results are predominantly driven by the incorporation of a nearly constant feeding interactions with increasing patch size and a realistic assumption for the extinction boundaries of populations

which is usually ignored in an ordinary differential equation modeling frameworks (e.g., *McCann, Rasmussen & Umbanhowar, 2005*; *Otto, Rall & Brose, 2007*). Future studies that aim to investigate effects of space on persistence using ordinary differential equation models should consider to include such more realistic extinction boundaries as presented in our study.

CONCLUSIONS

How species interactions react to environmental changes such as habitat homogenization and habitat loss is a key point for understanding how current global changes (*IPCC, 2014*) influence the stability and biodiversity of ecological networks. Increasing the stability of food webs is possible via obtaining weaker interaction strengths (*May, 1972*) which is important for maintaining biodiversity. We found that loss of habitat complexity would lead to increased interaction strength via decreasing half-saturation density. Additionally, even though the constant interaction strengths through different patch sizes lead to constant population densities, it would result in a less absolute number of individuals in smaller patches. When there are a reduced number of individuals in smaller patches, decreasing patch size would cause species extinctions, especially at higher trophic levels. Therefore, shrinking patch sizes and homogenizing habitats would both lead to destabilization of ecological networks and biodiversity loss. Altogether, our study underlines the urgent need for protecting large complex habitats to save biodiversity.

ACKNOWLEDGEMENTS

ADDITIONAL INFORMATION AND DECLARATIONS

Funding

Grant Disclosures

Competing Interests

The authors declare there are no competing interests.

Author Contributions

- Yuanheng Li conceived and designed the experiments, performed the experiments, analyzed the data, contributed reagents/materials/analysis tools, wrote the paper, prepared figures and/or tables, reviewed drafts of the paper.
- Ulrich Brose and Katrin Meyer conceived and designed the experiments, reviewed drafts of the paper.
- Björn C. Rall conceived and designed the experiments, analyzed the data, contributed reagents/materials/analysis tools, wrote the paper, reviewed drafts of the paper.

Data Availability

The following information was supplied regarding data availability:

The raw code has been supplied as a Supplementary File.

Supplemental Information

Supplemental information for this article can be found online at http://dx.doi.org/10.7717/peerj.2993#supplemental-information.

REFERENCES

Aljetlawi AA, Sparrevik E, Leonardsson K. 2004. Prey-predator size-dependent functional response: derivation and rescaling to the real world. *Journal of Animal Ecology* **73(2)**:239–252 DOI 10.1111/j.0021-8790.2004.00800.x.

Bergström U, Englund G. 2004. Spatial scale, heterogeneity and functional responses. *Journal of Animal Ecology* **73(3)**:487–493 DOI 10.1111/j.0021-8790.2004.00823.x.

Binzer A, Guill C, Rall BC, Brose U. 2016. Interactive effects of warming, eutrophication and size structure: impacts on biodiversity and food-web structure. *Global Change Biology* **22(1)**:220–227 DOI 10.1111/gcb.13086.

Boit A, Martinez ND, Williams RJ, Gaedke U. 2012. Mechanistic theory and modelling of complex food-web dynamics in Lake Constance. *Ecology Letters* **15(6)**:594–602 DOI 10.1111/j.1461-0248.2012.01777.x.

Bolker B, R Development Core Team. 2014. bbmle: Tools for general maximum likelihood estimation. R package version 1.0.17. *Available at https://cran.r-project.org/web/packages/bbmle/index.html*.

Bolker BM. 2008. *Ecological models and data in R*. Princeton: Princeton University Press.

Brose U. 2010. Body-mass constraints on foraging behaviour determine population and food-web dynamics. *Functional Ecology* **24(1)**:28–34 DOI 10.1111/j.1365-2435.2009.01618.x.

Brose U, Ehnes RB, Rall BC, Vucic-Pestic O, Berlow EL, Scheu S. 2008. Foraging theory predicts predator-prey energy fluxes. *Journal of Animal Ecology* **77(5)**:1072–1078 DOI 10.1111/j.1365-2656.2008.01408.x.

Brose U, Williams RJ, Martinez ND. 2006. Allometric scaling enhances stability in complex food webs. *Ecology Letters* **9(11)**:1228–1236 DOI 10.1111/j.1461-0248.2006.00978.x.

Brown JH, Gillooly JF, Allen AP, Savage VM, West GB. 2004. Toward a metabolic theory of ecology. *Ecology* **85(7)**:1771–1789 DOI 10.1890/03-9000.

Crawley MJ. 2007. *The R book*. Hoboken: Wiley.

Dale BW, Adams LG, Bowyer RT. 1994. Functional response of wolves preying on barren-ground caribou in a multiple-prey ecosystem. *Journal of Animal Ecology* **63(3)**:644–652 DOI 10.2307/5230.

De Ruiter PC, Neutel A-M, Moore JC. 1995. Energetics, patterns of interaction strengths, and stability in real ecosystems. *Science* **269(5228)**:1257–1260 DOI 10.1126/science.269.5228.1257.

Ebeling AW, Bray RN. 1976. Day versus night activity of reef fishes in a kelp forest off Santa Barbara, California. *Fishery Bulletin* **74(4)**:703–717.

Folsom TC, Collins NC. 1984. The diet and foraging behavior of the larval dragonfly Anax junius (Aeshnidae), with an assessment of the role of refuges and prey activity. *Oikos* **42(1)**:105–113 DOI 10.2307/3544615.

Fussmann KE, Schwarzmller F, Brose U, Jousset A, Rall BC. 2014. Ecological stability in response to warming. *Nature Climate Change* **4(3)**:206–210 DOI 10.1038/nclimate2134.

Gergs A. 2011. Modelling foraging behaviour in the insect predator Notonecta maculata using the individuals approach / vorgelegt von: Andrés Gergs. PhD thesis, RWTH Aachen University.

Gompertz B. 1825. On the nature of the function expressive of the law of human mortality, and on a new mode of determining the value of life contingencies. *Philosophical Transactions of the Royal Society of London* **115(0)**:513–583 DOI 10.1098/rstl.1825.0026.

Gotoh T, Nozawa M, Yamaguchi K. 2004. Prey consumption and functional response of three acarophagous species to eggs of the two-spotted spider mite in the laboratory. *Applied Entomology and Zoology* **39(1)**:97–105 DOI 10.1303/aez.2004.97.

Grimm V, Berger U, Bastiansen F, Eliassen S, Ginot V, Giske J, Goss-Custard J, Grand T, Heinz SK, Huse G, Huth A, Jepsen JU, Jørgensen C, Mooij WM, Müller B, Pe'er G, Piou C, Railsback SF, Robbins AM, Robbins MM, Rossmanith E, Rüger N, Strand E, Souissi S, Stillman RA, Visser U, DeAngelis DL. 2006. A standard protocol for describing individual-based and agent-based models. *Ecological Modelling* **198(1–2)**:115–126 DOI 10.1016/j.ecolmodel.2006.04.023.

Grimm V, Berger U, DeAngelis DL, Polhill JG, Giske J, Railsback SF. 2010. The ODD protocol: a review and first update. *Ecological Modelling* **221(23)**:2760–2768 DOI 10.1016/j.ecolmodel.2010.08.019.

Hauzy C, Tully T, Spataro T, Paul G, Arditi R. 2010. Spatial heterogeneity and functional response: an experiment in microcosms with varying obstacle densities. *Oecologia* **163(3)**:625–636 DOI 10.1007/s00442-010-1585-5.

Hoddle MS. 2003. The effect of prey species and environmental complexity on the functional response of *Franklinothrips orizabensis*: a test of the fractal foraging model. *Ecological Entomology* **28(3)**:309–318 DOI 10.1046/j.1365-2311.2003.00518.x.

Hohberg K, Traunspurger W. 2005. Predator-prey interaction in soil food web: functional response, size-dependent foraging efficiency, and the influence of soil texture. *Biology and Fertility of Soils* **41(6)**:419–427 DOI 10.1007/s00374-005-0852-9.

Holling CS. 1959a. The components of predation as revealed by a study of small-mammal predation of the European pine sawfly. *The Canadian Entomologist* **91(5)**:293–320 DOI 10.4039/Ent91293-5.

Holling CS. 1959b. Some characteristics of simple types of predation and parasitism. *The Canadian Entomologist* **91(7)**:385–398 DOI 10.4039/Ent91385-7.

Holling CS. 1966. The functional response of invertebrate predators to prey density. *Memoirs of the Entomological Society of Canada* **98(48)**:1–86 DOI 10.4039/entm9848fv.

Ibarrola I, Arambalza U, Navarro JM, Urrutia MB, Navarro E. 2012. Allometric relationships in feeding and digestion in the Chilean mytilids *Mytilus chilensis* (Hupé), *Choromytilus chorus* (Molina) and *Aulacomya ater* (Molina): a comparative study. *Journal of Experimental Marine Biology and Ecology* **426–427**:18–27 DOI 10.1016/j.jembe.2012.05.012.

IPCC. 2014. Field CB, Barros VR, Dokken DJ, Mach KJ, Mastrandrea MD, Bilir TE, Chatterjee M, Ebi KL, Estrada YO, Genova RC, Girma B, Kissel ES, Levy AN, MacCracken S, Mastrandrea PR, White LL, eds. *Climate change 2014: impacts, adaptation, and vulnerability. Part a: global and sectoral aspects. Contribution of working group ii to the fifth assessment report of the intergovernmental panel on climate change.* Cambridge: Cambridge University Press.

Jeschke JM, Kopp M, Tollrian R. 2002. Predator functional responses: discriminating between handling and digesting prey. *Ecological Monographs* **72(1)**:95–112 DOI 10.2307/3100087.

Jeschke JM, Kopp M, Tollrian R. 2004. Consumer-food systems: why type I functional responses are exclusive to filter feeders. *Biological Reviews of the Cambridge Philosophical Society* **79(2)**:337–349.

Juliano SA. 2001. Non-linear curve fitting: predation and functional response curves. In: Scheiner SM, Gurevitch J, eds. *Design and analysis of ecological experiments.* 2nd edition. New York: Oxford University Press, 178–196.

Kaiser H. 1983. Small scale spatial heterogeneity influences predation success in an unexpected way: model experiments on the functional response of predatory mites (Acarina). *Oecologia* **56(2–3)**:249–256 DOI 10.1007/BF00379698.

Kalinkat G, Brose U, Rall BC. 2013. Habitat structure alters top-down control in litter communities. *Oecologia* **172(3)**:877–887 DOI 10.1007/s00442-012-2530-6.

Kalinkat G, Rall BC. 2015. Effects of climate change on the interactions between insect pests and their natural enemies. In: Björkman C, Niemelä P, eds. *Climate change and insect pests.* Wallingford: CABI, 74–91.

Kalinkat G, Schneider FD, Digel C, Guill C, Rall BC, Brose U. 2013. Body masses, functional responses and predator-prey stability. *Ecology Letters* **16(9)**:1126–1134 DOI 10.1111/ele.12147.

Kleiber M. 1961. *The fire of life: an introduction to animal energetics.* New York: Wiley.

Lotka AJ. 1925. *Elements of physical biology.* Baltimore: Williams and Wilkins Company.

MacArthur R. 1955. Fluctuations of animal populations and a measure of community stability. *Ecology* **36(3)**:533–536 DOI 10.2307/1929601.

May RM. 1972. Will a large complex system be stable?. *Nature* **238(5364)**:413–414 DOI 10.1038/238413a0.

McCann KS. 2000. The diversity–stability debate. *Nature* **405(6783)**:228–233 DOI 10.1038/35012234.

McCann KS, Rasmussen JB, Umbanhowar J. 2005. The dynamics of spatially coupled food webs: spatially coupled food webs. *Ecology Letters* **8(5)**:513–523 DOI 10.1111/j.1461-0248.2005.00742.x.

Meehan TD. 2006. Energy use and animal abundance in litter and soil communities. *Ecology* **87(7)**:1650–1658.

Miller JRB, Ament JM, Schmitz OJ. 2014. Fear on the move: predator hunting mode predicts variation in prey mortality and plasticity in prey spatial response. *Journal of Animal Ecology* **83(1)**:214–222 DOI 10.1111/1365-2656.12111.

Munyaneza J, Obrycki JJ. 1997. Functional response of *Coleomegilla maculata* (Coleoptera: Coccinellidae) to colorado potato beetle eggs (Coleoptera: Chrysomelidae). *Biological Control* **8(3)**:215–224 DOI 10.1006/bcon.1997.0509.

Murdoch WW, Oaten A. 1975. Predation and population stability, In: MacFadyen A, ed. *Advances in ecological research.* Vol. 9. Cambridge: Academic Press, 1–131.

Nunney L. 1980a. The influence of the type 3 (sigmoid) functional response upon the stability of predator-prey difference models. *Theoretical Population Biology* **18(2)**:257–278 DOI 10.1016/0040-5809(80)90052-0.

Nunney L. 1980b. The stability of complex model ecosystems. *The American Naturalist* **115(5)**:639–649 DOI 10.1086/283589.

Oaten A, Murdoch WW. 1975. Switching, functional response, and stability in predator-prey systems. *The American Naturalist* **109(967)**:299–318.

Otto SB, Rall BC, Brose U. 2007. Allometric degree distributions facilitate food-web stability. *Nature* **450(7173)**:1226–1229 DOI 10.1038/nature06359.

Persson A, Brönmark C. 2002a. Foraging capacities and effects of competitive release on ontogenetic diet shift in bream, *Abramis brama*. *Oikos* **97(2)**:271–281 DOI 10.1034/j.1600-0706.2002.970213.x.

Persson A, Brönmark C. 2002b. Foraging capacity and resource synchronization in an ontogenetic diet switcher, Pikeperch (*Stizostedion lucioperca*). *Ecology* **83(11)**:3014–3022 DOI 10.1890/0012-9658(2002)083[3014:FCARSI]2.0.CO;2.

Persson L, Leonardsson K, De Roos AM, Gyllenberg M, Christensen B. 1998. Ontogenetic scaling of foraging rates and the dynamics of a size-structured consumer-resource model. *Theoretical Population Biology* **54(3)**:270–293 DOI 10.1006/tpbi.1998.1380.

Peters RH. 1983. The ecological implications of body size. In: *Number 2 in Cambridge studies in ecology*. repr edition. New York: Cambridge University Press.

R Core Team. 2016. R: a language and environment for statistical computing. Vienna: R Foundation for Statistical Computing. *Available at https://www.r-project.org/*.

Rall BC, Brose U, Hartvig M, Kalinkat G, Schwarzmuller F, Vucic-Pestic O, Petchey OL. 2012. Universal temperature and body-mass scaling of feeding rates. *Philosophical Transactions of the Royal Society B: Biological Sciences* **367**(**1605**):2923–2934 DOI 10.1098/rstb.2012.0242.

Rall BC, Guill C, Brose U. 2008. Food-web connectance and predator interference dampen the paradox of enrichment. *Oikos* **117**(**2**):202–213 DOI 10.1111/j.2007.0030-1299.15491.x.

Rall BC, Kalinkat G, Ott D, Vucic-Pestic O, Brose U. 2011. Taxonomic versus allometric constraints on non-linear interaction strengths. *Oikos* **120**(**4**):483–492 DOI 10.1111/j.1600-0706.2010.18860.x.

Rall BC, Vucic-Pestic O, Ehnes RB, Emmerson M, Brose U. 2010. Temperature, predator-prey interaction strength and population stability. *Global Change Biology* **16**(**8**):2145–2157 DOI 10.1111/j.1365-2486.2009.02124.x.

Real LA. 1977. The kinetics of functional response. *The American Naturalist* **111**(**978**): 289–300 DOI 10.1086/283161.

Rosenzweig ML. 1971. Paradox of enrichment: destabilization of exploitation ecosystems in ecological time. *Science* **171**(**3969**):385–387 DOI 10.1126/science.171.3969.385.

Rosenzweig ML, MacArthur RH. 1963. Graphical representation and stability conditions of predator-prey interactions. *The American Naturalist* **97**(**895**):209–223.

Sarnelle O, Wilson AE. 2008. Type III functional response in Daphnia. *Ecology* **89**(**6**):1723–1732.

Savage VM, Gilloly JF, Brown JH, Charnov EL. 2004a. Effects of body size and temperature on population growth. *The American Naturalist* **163**(**3**):429–441 DOI 10.1086/381872.

Savage VM, Gillooly JF, Woodruff WH, West GB, Allen AP, Enquist BJ, Brown JH. 2004b. The predominance of quarter-power scaling in biology. *Functional Ecology* **18**(**2**):257–282 DOI 10.1111/j.0269-8463.2004.00856.x.

Scheffer M, De Boer RJ. 1995. Implications of spatial heterogeneity for the paradox of enrichment. *Ecology* **76**(**7**):2270–2277 DOI 10.2307/1941701.

Schmitz OJ, Krivan V, Ovadia O. 2004. Trophic cascades: the primacy of trait-mediated indirect interactions. *Ecology Letters* **7**(**2**):153–163 DOI 10.1111/j.1461-0248.2003.00560.x.

Schneider FD, Brose U, Rall BC, Guill C. 2016. Animal diversity and ecosystem functioning in dynamic food webs. *Nature Communications* **7**:12718 DOI 10.1038/ncomms12718.

Schneider FD, Scheu S, Brose U. 2012. Body mass constraints on feeding rates determine the consequences of predator loss. *Ecology Letters* **15**(**5**):436–443 DOI 10.1111/j.1461-0248.2012.01750.x.

Smout S, Lindstrøm U. 2007. Multispecies functional response of the minke whale *Balaenoptera acutorostrata* based on small-scale foraging studies. *Marine Ecolog-Progress Series* **341**:277–291 DOI 10.3354/meps341277.

Verhulst P. 1838. Notice sur la loi que la population suit dans son accroissement. *Correspondance Mathëmatique et Physique* **10**:113–121.

Volterra V. 1926. Fluctuations in the abundance of a species considered mathematically. *Nature* **118(2972)**:558–560 DOI 10.1038/118558a0.

Vucic-Pestic O, Birkhofer K, Rall BC, Scheu S, Brose U. 2010a. Habitat structure and prey aggregation determine the functional response in a soil predator-prey interaction. *Pedobiologia* **53(5)**:307–312 DOI 10.1016/j.pedobi.2010.02.003.

Vucic-Pestic O, Ehnes RB, Rall BC, Brose U. 2011. Warming up the system: higher predator feeding rates but lower energetic efficiencies. *Global Change Biology* **17(3)**:1301–1310 DOI 10.1111/j.1365-2486.2010.02329.x.

Vucic-Pestic O, Rall BC, Kalinkat G, Brose U. 2010b. Allometric functional response model: body masses constrain interaction strengths. *Journal of Animal Ecology* **79(1)**:249–256 DOI 10.1111/j.1365-2656.2009.01622.x.

Wahlström E, Persson L, Diehl S, Byström P. 2000. Size-dependent foraging efficiency, cannibalism and zooplankton community structure. *Oecologia* **123(1)**:138–148 DOI 10.1007/s004420050999.

Williams RJ, Martinez ND. 2004. Stabilization of chaotic and non-permanent food-web dynamics. *The European Physical Journal B—Condensed Matter* **38(2)**:297–303 DOI 10.1140/epjb/e2004-00122-1.

Yodzis P. 1981. The stability of real ecosystems. *Nature* **289(5799)**:674–676 DOI 10.1038/289674a0.

Yodzis P, Innes S. 1992. Body size and consumer-resource dynamics. *The American Naturalist* **139(6)**:1151–1175 DOI 10.1086/285380.

Zuur AF, Ieno EN, Walker N, Saveliev AA, Smith GM. 2009. Mixed effects models and extensions in ecology with R. *Statistics for biology and health*, New York: Springer New York.